

REPORT DOCUMENTATION PAGE			Form Approved OMB NO. 0704-0188		
<p>The public reporting burden for this collection of information is estimated to average 1 hour per response, including the time for reviewing instructions, searching existing data sources, gathering and maintaining the data needed, and completing and reviewing the collection of information. Send comments regarding this burden estimate or any other aspect of this collection of information, including suggestions for reducing this burden, to Washington Headquarters Services, Directorate for Information Operations and Reports, 1215 Jefferson Davis Highway, Suite 1204, Arlington VA, 22202-4302. Respondents should be aware that notwithstanding any other provision of law, no person shall be subject to any penalty for failing to comply with a collection of information if it does not display a currently valid OMB control number. PLEASE DO NOT RETURN YOUR FORM TO THE ABOVE ADDRESS.</p>					
1. REPORT DATE (DD-MM-YYYY) 12-07-2023		2. REPORT TYPE Final Report		3. DATES COVERED (From - To) 1-Mar-2019 - 28-Feb-2023	
4. TITLE AND SUBTITLE Final Report: Multiblock Copolymers with Sulfonated Poly (arylene ethers) and Fluoropolymers for Improved Protective Capabilities and Energy Efficient Devices			5a. CONTRACT NUMBER W911NF-19-1-0093		
			5b. GRANT NUMBER		
			5c. PROGRAM ELEMENT NUMBER 611102		
6. AUTHORS			5d. PROJECT NUMBER		
			5e. TASK NUMBER		
			5f. WORK UNIT NUMBER		
7. PERFORMING ORGANIZATION NAMES AND ADDRESSES University of Puerto Rico at Mayaguez Call Box 9000 Mayaguez, PR 00681 -9000			8. PERFORMING ORGANIZATION REPORT NUMBER		
9. SPONSORING/MONITORING AGENCY NAME(S) AND ADDRESS (ES) U.S. Army Research Office P.O. Box 12211 Research Triangle Park, NC 27709-2211			10. SPONSOR/MONITOR'S ACRONYM(S) ARO		
			11. SPONSOR/MONITOR'S REPORT NUMBER(S) 72970-SM.7		
12. DISTRIBUTION AVAILABILITY STATEMENT Approved for public release; distribution is unlimited					
13. SUPPLEMENTARY NOTES The views, opinions and/or findings contained in this report are those of the author(s) and should not be construed as an official Department of the Army position, policy or decision, unless so designated by other documentation.					
14. ABSTRACT					
15. SUBJECT TERMS					
16. SECURITY CLASSIFICATION OF:		17. LIMITATION OF ABSTRACT		15. NUMBER OF PAGES	19a. NAME OF RESPONSIBLE PERSON
a. REPORT UU	b. ABSTRACT UU	c. THIS PAGE UU	UU		David Suleiman
					19b. TELEPHONE NUMBER 787-832-4040

RPPR Final Report

as of 12-Jul-2023

Agency Code: 21XD

Proposal Number: 72970SM

Agreement Number: W911NF-19-1-0093

INVESTIGATOR(S):

Name: Ph.D. David Suleiman dsuleiman@

Email: david.suleiman@upr.edu

Phone Number: 7878324040

Principal: Y

Organization: **University of Puerto Rico at Mayaguez**

Address: Call Box 9000, Mayaguez, PR 006819000

Country: USA

DUNS Number: 175303262

EIN: 660433761

Report Date: 31-May-2023

Date Received: 12-Jul-2023

Final Report for Period Beginning 01-Mar-2019 and Ending 28-Feb-2023

Title: Multiblock Copolymers with Sulfonated Poly (arylene ethers) and Fluoropolymers for Improved Protective Capabilities and Energy Efficient Devices

Begin Performance Period: 01-Mar-2019

End Performance Period: 28-Feb-2023

Report Term: 0-Other

Submitted By: Ph.D. David Suleiman

Email: david.suleiman@upr.edu

Phone: (787) 832-4040

Distribution Statement: 2-Distribution Limited to U.S. Government agencies only; report contains proprietary information

STEM Degrees: 16

STEM Participants: 17

Major Goals: The work outlined in this report describes the synthesis and characterization of multi-block copolymers, based on robust aromatic backbones with multi-ionic domains, to create exclusive architectures and functionalities. The goal is to provide a fundamental understanding of the unique polymer chemistry, nanostructure, and the resulting structure-property relationship of the materials. Condensation polymerization and atom transfer radical polymerization (ATRP) has been used to create multi-block copolymers using different ionic domains (i.e. sulfones, ketones, sulfonated, ethers, and fluoropolymers), with distinctive block composition, in order to develop unique chemical architectures. The nanostructure of the resulting polymers have been critically evaluated using a combination of chemical (EA, FT-IR), thermal (TGA, DSC), mechanical (AFM), and morphological (SAXS) characterization techniques. The novel polymer architectures also incorporated counter-ions in specific ionic domains to create selective polymer metal nanocomposite membranes (PMNM).

Although the focus of this research project is on basic research and advancing the fundamental understanding of nanostructured polymers, these materials have very important applications for the Department of Defense (DoD). In the area of chemical and biological protective clothing (CBPC), sulfonated PMNMs have been used to reduce the permeation of a simulant to Sarin gas (DMMP) by at least one order of magnitude over water. The unique chemical and morphological nanostructure of the proposed PMNM, with selective multi-ionic domains, exacerbated the difference in transport properties even further for this and other chemicals and biological toxins, thus enhancing the protection of soldiers. Similarly, in the area of direct methanol fuel cells (DMFC), where sulfonated polymers have been found to be more selective (transport of protons over methanol) as compared to the state-of-the-art Nafion, the fundamental understanding between polymer chemistry and morphology could further enhance the transport of protons over methanol. This would, therefore, advance the development of more energy-efficient devices to provide power to soldiers in remote locations. Finally, the proposed polymers have numerous potential applications in other electrochemical/chemical devices, which could provide soldiers with a lightweight energy alternative during their military operations.

Accomplishments: Two technical peer-reviewed publications have been published, while the third publication is being submitted and evaluated. Seven technical presentations were presented in local and national conferences. One underrepresented Hispanic student completed his Ph.D in Chemical Engineering and 15 undergraduate BS

RPPR Final Report as of 12-Jul-2023

students in Chemical Engineering learned about Polymer Chemistry, material characterization, and Transport studies, while completing their degrees.

Sulfonated poly(arylene ether sulfone) (SPAES) and sulfonated poly(arylene ether ketone) (SPAEK) were synthesized using low-temperature coupling of hydrophilic and hydrophobic blocks and random polymerization. Unique ionic synergistic effects were observed for SPAES producing proton conductivities over twice as the state-of-the-art Nafion®. SPAEK showed remarkable oxidative stability and extremely low permeability due its resulting morphology and ionic interconnections.

Training Opportunities: Underrepresented Hispanic students were trained on: Polymer Chemistry, material characterization (FT-IR, UV, TGA, AFM, SAXS/WAXS), and Transport studies (vapor and liquid permeabilities and proton conductivity).

Results Dissemination: Two technical peer-reviewed publications have been published, while the third publication is being submitted and evaluated. Seven technical presentations were presented in local and national conferences. One underrepresented Hispanic student completed his Ph.D in Chemical Engineering and 15 undergraduate BS students in Chemical Engineering learned about Polymer Chemistry, material characterization, and Transport studies, while completing their degrees.

Honors and Awards: Honors and Awards for Professor David Suleiman - PI for this award

1. James Y. Oldshue Lecture, AIChE National Meeting, AIChE, Phoenix, AZ (November 2022).
2. Distinguished Professor of Chemical Engineering, University of Puerto Rico, Mayaguez, PR (May, 2022).
3. Eminem Chemical Engineer Award, Minority Affairs Committee, AIChE (November, 2020).

Protocol Activity Status:

Technology Transfer: Nothing to Report

PARTICIPANTS:

Participant Type: PD/PI

Participant: David Suleiman

Person Months Worked: 1.00

Project Contribution:

National Academy Member: N

Funding Support:

Participant Type: Graduate Student (research assistant)

Participant: Gilberto Ramos-Rivera

Person Months Worked: 12.00

Project Contribution:

National Academy Member: N

Funding Support:

Participant Type: Graduate Student (research assistant)

Participant: Juan Rivera-Diaz

Person Months Worked: 3.00

Project Contribution:

National Academy Member: N

Funding Support:

Participant Type: Undergraduate Student

Participant: Jesus Melendez

RPPR Final Report
as of 12-Jul-2023

Person Months Worked: 6.00
Project Contribution:
National Academy Member: N

Funding Support:

Participant Type: Undergraduate Student
Participant: Alanis Olmo
Person Months Worked: 12.00
Project Contribution:
National Academy Member: N

Funding Support:

Participant Type: Undergraduate Student
Participant: Sylvette Pagan
Person Months Worked: 6.00
Project Contribution:
National Academy Member: N

Funding Support:

Participant Type: Undergraduate Student
Participant: Guillermo Sotomayor
Person Months Worked: 12.00
Project Contribution:
National Academy Member: N

Funding Support:

Participant Type: Undergraduate Student
Participant: Maria Torres
Person Months Worked: 6.00
Project Contribution:
National Academy Member: N

Funding Support:

Participant Type: Undergraduate Student
Participant: Adrian Gonzalez
Person Months Worked: 6.00
Project Contribution:
National Academy Member: N

Funding Support:

Participant Type: Undergraduate Student
Participant: Veronica Martinez
Person Months Worked: 6.00
Project Contribution:
National Academy Member: N

Funding Support:

Participant Type: Undergraduate Student
Participant: Yadeiris Nieves
Person Months Worked: 6.00
Project Contribution:

Funding Support:

RPPR Final Report
as of 12-Jul-2023

National Academy Member: N

Participant Type: Undergraduate Student

Participant: Melanie Albarran

Person Months Worked: 6.00

Project Contribution:

National Academy Member: N

Funding Support:

Participant Type: Undergraduate Student

Participant: Dariana Giusti

Person Months Worked: 12.00

Project Contribution:

National Academy Member: N

Funding Support:

Participant Type: Undergraduate Student

Participant: Kevin Correa

Person Months Worked: 6.00

Project Contribution:

National Academy Member: N

Funding Support:

Participant Type: Undergraduate Student

Participant: Marcos Fragela

Person Months Worked: 6.00

Project Contribution:

National Academy Member: N

Funding Support:

Participant Type: Undergraduate Student

Participant: Alanis Matías

Person Months Worked: 6.00

Project Contribution:

National Academy Member: N

Funding Support:

Participant Type: Undergraduate Student

Participant: Sonyalee Soto

Person Months Worked: 3.00

Project Contribution:

National Academy Member: N

Funding Support:

Participant Type: Undergraduate Student

Participant: Paola Mendez

Person Months Worked: 6.00

Project Contribution:

National Academy Member: N

Funding Support:

RPPR Final Report
as of 12-Jul-2023

ARTICLES:

Publication Type: Journal Article Peer Reviewed: Y **Publication Status:** 1-Published

Journal: Journal of Applied Polymer Science

Publication Identifier Type: DOI

Publication Identifier: <https://doi.org/10.1002/app.50034>

Volume: 138

Issue: 11

First Page #: 1

Date Submitted: 8/29/21 12:00AM

Date Published: 10/16/20 4:00AM

Publication Location:

Article Title: Chemical and morphological effects of blended sulfonated poly(styrene-isobutylene-styrene) and isopentylamine for direct methanol fuel cell applications

Authors: Karen Barrios-Tarazona, David Suleiman

Keywords: acid-base interaction, direct methanol fuel cell, morphology, proton exchange membrane, transport properties

Abstract: In this study, blend membranes based on a combination of sulfonated poly (styrene-isobutylene-styrene) (SIBS) with isopentylamine (IPA) were synthesized as potential candidates for direct methanol fuel cell (DMFC) applications. The impact of sulfonation level (57–93 mol%) and percentage of IPA incorporation (1, 3, and 5 wt%) were analyzed via different properties of the resulting membrane. FTIR analysis showed that IPA was successfully incorporated into the sulfonated polymer matrix and also confirmed the interaction between the sulfonic and amine groups. This interaction generates significant morphological changes in the nanostructure of the membranes that are evident through results of small angle x-ray scattering and atomic force microscopy analysis. Proton conductivity and methanol permeability of the membranes were also analyzed. Proton conductivity was significantly enhanced with the incorporation of IPA at an optimum loading, creating additional paths for the conduction of protons.

Distribution Statement: 1-Approved for public release; distribution is unlimited.

Acknowledged Federal Support: Y

Publication Type: Journal Article Peer Reviewed: Y **Publication Status:** 1-Published

Journal: Journal of Polymer Science

Publication Identifier Type: DOI

Publication Identifier: <https://doi.org/10.1002/pol.20210214>

Volume:

Issue:

First Page #:

Date Submitted: 8/29/21 12:00AM

Date Published: 7/1/21 4:00AM

Publication Location:

Article Title: Sulfonated poly(styrene-isobutylene-styrene) grafted with hexyl- and butyl-imidazolium chloride ionic liquids

Authors: Karen Barrios-Tarazona, David Suleiman

Keywords: chemical grafting, chemical protective clothing, membrane gas separations, sulfonated PIL's membranes

Abstract: In this work, novel sulfonated poly(ionic liquid)s block-copolymers based on poly(styrene-isobutylene-styrene) (SIBS) are synthesized for chemical protective clothing (CPC) applications. The synthesis consists of the chloromethylation of SIBS, followed by the incorporation of N-alkylimidazole through chemical grafting, and concluding with sulfonation of the resulting compound. Properties of the membranes are determined as a function of different N-alkylimidazoles (butylimidazole and hexylimidazole) and sulfonation levels (7–23 mol%). Results show that the incorporation of imidazole and sulfonic groups increases the thermal stability of SIBS as well as its water absorption capabilities. The interaction between the ionic moieties in the polymeric matrix allows the formation of hydrophilic nanochannels, which promote the transport of permeants through the membrane. The high water vapor transmission rate (above 2000 g m⁻² day⁻¹) and values of selectivity (~50) demonstrate that the breathability is improved.

Distribution Statement: 1-Approved for public release; distribution is unlimited.

Acknowledged Federal Support: Y

RPPR Final Report as of 12-Jul-2023

Publication Type: Journal Article Peer Reviewed: Y **Publication Status:** 1-Published

Journal: Journal of Applied Polymer Science

Publication Identifier Type: DOI

Publication Identifier: doi.org/10.1002/app.52027

Volume: 139

Issue: 17

First Page #: 52027

Date Submitted: 8/18/22 12:00AM

Date Published: 12/13/21 4:00AM

Publication Location:

Article Title: High-Performance Blend Membranes Based on Poly(arylene ether sulfone) and Poly(styrene-isobutylene-styrene) for Direct Methanol Fuel Cell Applications

Authors: Gilberto Ramos-Rivera, David Suleiman

Keywords: Hydrophilic-Hydrophobic Blocks, Sulfonation, DMFC, Blends

Abstract: In this study, two series of poly(arylene ether sulfone)s (PAES) with hydrophobic blocks made of 4,4'-Dihydroxyphenyl (BP) and 2,2-Bis(4-hydroxyphenyl) propane (BPA) were synthesized. The copolymers were prepared by a coupling reaction between decafluorobiphenyl (DFBP) end-capped non-sulfonated block (PAES A or B) and sulfonated block (SPAES B). The reactive behavior of DFBP facilitates the low-temperature coupling reaction (below 105 °C). The final copolymers were blended at distinct weight percent ratios (0, 20, 30, 40) with poly(styrene-*b*-isobutylene-*b*-styrene) (SIBS) at a sulfonation level of 88% to obtain strong and flexible membranes. Morphological, thermal stability and conduction properties of the resulting membranes were measured and reported here. Results suggest that phase segregation between hydrophobic and hydrophilic domains occurs below 1 meq. g⁻¹ IEC. These membranes have low water absorption and high thermal stability. Incorporating SIBS 88 into the blend added elast

Distribution Statement: 2-Distribution Limited to U.S. Government agencies only; report contains proprietary info
Acknowledged Federal Support: Y

Publication Type: Journal Article Peer Reviewed: Y **Publication Status:** 1-Published

Journal: Journal of Applied Polymer Science

Publication Identifier Type: DOI

Publication Identifier: 10.1002/app.53595

Volume: 140

Issue: 10

First Page #: 1

Date Submitted: 7/12/23 12:00AM

Date Published: 1/4/23 4:00AM

Publication Location:

Article Title: Synthesis and characterization of multi-ionic block copolymers and blended membranes for chemical protective clothing applications

Authors: Karen Barrios Tarazona, Gilberto Ramos-Rivera, David Suleiman

Keywords: blends, copolymers, membranes, nanostructured polymers, thermogravimetric analysis (TGA)

Abstract: This study discusses the synthesis of sulfonated amine block copolymers and the effect of multiple ionic domains and counter-ion substitution on polymeric membranes' morphology and transport properties for chemical protective clothing (CPC) applications. The monomers 2-(tert-butylamino) ethyl methacrylate, 2-ethoxy ethyl methacrylate, and styrene were used to prepare the block copolymers by atom transfer radical polymerization (ATRP). The copolymers were then sulfonated by chemical grafting with pendants sulfobutyl groups onto the polymer structure. Properties of the resulting membranes were evaluated as a function of block composition, incorporation of sulfonic groups, and counter-ion substitution. Blended membranes with sulfonated poly(styrene-isobutylene-styrene) (SIBS) were also studied. A series of materials characterization techniques (e. g., Fourier-transform infrared spectroscopy [FT-IR], thermogravimetric analysis [TGA], atomic force microscopy [AFM], SAXS

Distribution Statement: 1-Approved for public release; distribution is unlimited.

Acknowledged Federal Support: Y

RPPR Final Report as of 12-Jul-2023

Publication Type: Journal Article Peer Reviewed: Y **Publication Status:** 1-Published

Journal: Journal of Applied Polymer Science

Publication Identifier Type: DOI

Publication Identifier: 10.1002/app.52027

Volume: 139

Issue: 17

First Page #: 1

Date Submitted: 7/12/23 12:00AM

Date Published: 12/13/21 4:00AM

Publication Location:

Article Title: High-performance blended membranes based on poly(arylene ether sulfone) and sulfonated poly(styrene-isobutylene-styrene) for direct methanol fuel cell applications

Authors: Gilberto Ramos-Rivera, David Suleiman

Keywords: blends, conducting polymers, copolymers, membranes

Abstract: In this study, two series of poly(arylene ether sulfone)s (PAES) with hydrophobic blocks made of 4,4'-dihydroxyphenyl (BP) and 2,2-bis(4-hydroxyphenyl) propane (BPA) were synthesized. The copolymers were prepared by a coupling reaction between decafluorobiphenyl (DFBP) end-capped nonsulfonated block (PAES A or B) and sulfonated block (SPAES B). The reactive behavior of DFBP facilitates the low-temperature coupling reaction (below 105°C). The final copolymers were blended at distinct weight percent ratios (0, 20, 30, and 40) with poly(styrene-*b*-isobutylene-*b*-styrene) (SIBS) at a sulfonation level of 88% to obtain strong and flexible membranes. Morphological, thermal stability, and conduction properties of the resulting membranes were measured and reported here. Results suggest that phase segregation between hydrophobic and hydrophilic domains occurs below 1 meq. g⁻¹ ion exchange capacity. These membranes have low water absorption and high thermal stability. Incorporating SIBS 88 into th

Distribution Statement: 1-Approved for public release; distribution is unlimited.

Acknowledged Federal Support: Y

DISSERTATIONS:

Publication Type: Thesis or Dissertation

Institution: University of Puerto Rico at Mayaguez

Date Received: 29-Aug-2021

Completion Date: 7/7/21 8:13PM

Title: SYNTHESIS AND CHARACTERIZATION OF SULFONATED AMINE BLOCK COPOLYMER MEMBRANES FOR FUEL CELLS AND SPECIALTY SEPARATIONS APPLICATIONS

Authors: Karen A. Barrios-Tarazona

Acknowledged Federal Support: Y

Partners

I certify that the information in the report is complete and accurate:

Signature: David Suleiman

Signature Date: 7/12/23 9:03AM

Multiblock Copolymers with Sulfonated Poly(arylene-ethers) and Fluoropolymers for Improved Protective Capabilities and Energy Efficient Devices

Final Progress Report: Scientific Progress and Accomplishments

01 Aug 2022 – 28 Feb 2023, David Suleiman, PI (University of Puerto Rico at Mayaguez), W911NF-19-1-0093

Abstract

During this project one Ph.D. student and fifteen undergraduate (B.S.) students worked on this investigation. This work focused on the synthesis and characterization of multiblock copolymers composed of sulfonated poly(arylene ether sulfones) (SPAES) and sulfonated poly(arylene ether ketones) (SPAEK) for fuel cell and chemical protective clothing (CPC) applications. Low-temperature coupling of hydrophilic and hydrophobic blocks was used, with emphasis on evaluating different ionic domains with adequate elastomeric domains to achieve membrane barrier properties. First we published an article that described how the synergistic effects of sulfonic, sulfones and ether domains produced proton conductivities of 0.22 S/cm at 50° C; twice as much as the state-of-the-art Nafion®. We then tried to incorporate a pentafluorostyrene block to SPAES using ATRP. Unfortunately, phase segregation did not allow us to obtain proper membranes, even as we evaluated different block compositions. Different multi-ionic blocks were synthesized using ATRP and a second paper was published on highly selective membranes, but for CPC applications. Finally, the focus of this report, and the third publication, aimed at the synthesis and characterization of SPAES and SPAEK. The results produced membranes with high proton conductivity (0.24 S/cm at 80° C) for SPAES, while SPAEK produced extremely low methanol permeability and excellent oxidative stability. Future studies are proposed on the use of SPAEKS.

1.0 Introduction

Proton exchange membranes (PEMs) have been one of the most important components in the development of fuel cells, including direct methanol fuel cells (DMFC). These ionic membranes serve a dual function acting as a conductor matrix for protons and an insulator barrier for the fuel. For decades much of the PEM research has focused on the preparation of electrolytic membranes with the ability to surpass the state-of-the-art Nafion[®]. Common disadvantages associated with Nafion[®] are its high methanol crossover, an elevated price, and processability issues because of its perfluorinated nature.¹

Among the materials proposed as candidates for Nafion[®] replacement, poly(arylene ethers) stand out. These materials possess high thermal stability, good oxidative stability, and elevated solvent resistance.² Even though the previous advantages make them attractive PEM candidates, the proton conductivity, which is an essential factor to be addressed hasn't been fully explored. Sulfonation has been the most important ionic domain as the most conductive membranes contain sulfonic domains. Sulfonation can be achieved by pre- or post-sulfonation processes. Post-sulfonation methods are extensively published in the literature, and they commonly employ a sulfonating agent to attach sulfonic groups to specific sites in the polymer structure. Numerous studies support the easy sulfonation results obtained using this method; however, they also raise a red flag about the difficulty of controlling the sulfonation level. This difficulty could be due to steric effects surrounding the desired sulfonation location or potential side reactions. For example, it has been reported that for the post-sulfonation process of poly(arylene ether

sulfones) (PAES), high sulfonation levels could provoke undesired reactions such as chain scissoring and crosslinks.³

Compared with the post-sulfonation approach, pre-sulfonation is an effective way to obtain specific polymers by reacting sulfonated monomers with other desired moieties. This methodology was first developed by Ueda et al. in the 1990s.⁴ Their work use sodium 5,5'-sulfonylbis (2-chlorobenzene sulfonate) (SDCDPS), a polymer previously developed by Robeson.⁴ Years later, McGrath and his coworkers improved the purity of this sulfonated unit and achieved higher molecular weights with systems of up to 100% degree of sulfonation by increasing the reaction temperature to 190 °C.⁵⁻⁷ Recent studies show the remarkable employment of sulfonated and non-sulfonated units as copolymers for PEM applications. Pirali-Hamedani & Mehdipour-Ataei reported the synthesis of hydroquinone and 4,4'-(4,4'-sulfonyl bis-(1,4-phenylene)bis(oxy)) diphenol based on PAES. Their results indicate that polymers with larger repeating unit sizes were better candidates for PEMs; however, their proton conductivity values were below 0.1 S cm⁻¹,⁸ considered a standard value from the state-of-the-art Nafion® at 50 °C. In 2016, Wang et al. reported the synthesis of a copolymer based on a dual naphthalene and flexible sulfoalkyl groups, achieving a conductivity of 0.271 S cm⁻¹ at 80 °C.⁹ In addition, Liu et al. prepared a series of poly(arylene ether ketone)s (PAEK) with grafted 1,4 butanesultone. This particular comb-shaped polymer obtained conductivities of 0.101 S cm⁻¹ at 80 °C, while methanol permeabilities were between 7.56 x10⁻⁷ to 9.44 x10⁻⁷ cm² s⁻¹, which is highly desirable for DMFC applications.¹⁰

The following work synthesized and characterized two sulfonated poly(arylene ether) series based on sulfone and ketone units. The polymers were created to achieve a random structure, starting with a pre-sulfonated unit.

2.0 Experimental Procedure

2.1 Materials

4,4'-Dichlorobiphenyl sulfone (DCDPS) 98.0+% and 2,2-Bis(4-hydroxyphenyl) propane (BPA) 99.0+% were obtained from TCL America™ and dried at 60 °C prior to use. N, N-dimethylacetamide (DMAc) 99% pure, 2-Propanol (IPA) 99.5%, Sulfuric acid (20% fuming, 18-24% free SO₃), and 4,4'-Dichlorobenzophenone (DCBP) (99%) were purchased from Alfa Aesar™ and used without further purification. Toluene (ACS grade), Methanol (99.8%, Extra Dry), and Sulfuric acid (ACS grade) were obtained from Fisher Scientific™, and Potassium carbonate (K₂CO₃) was 98% pure from Acros Organics™.

2.2 Methodology

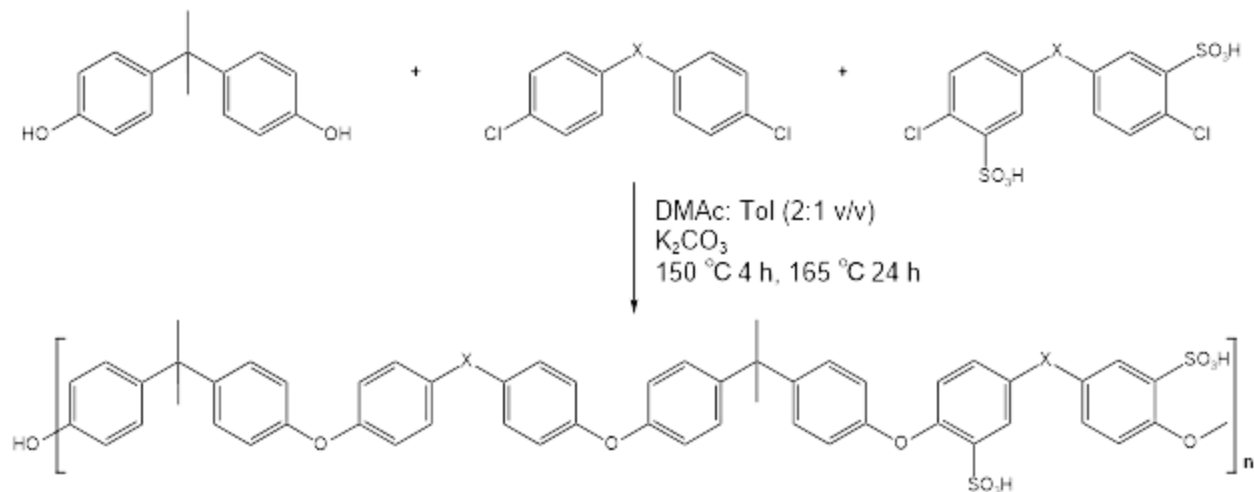
2.2.1 Synthesis of Sulfonated Unit

To a 250 mL three-necked flask with a nitrogen inlet/outlet, 28.7 g of DCDPS or DCBP was added and dissolved in 60 mL of fuming sulfuric acid. The solution was heated to 110 °C for 6 hours. The reaction mixture was cooled to room temperature, and 400 ml of cold water was added. Then, 180 g of NaCl was added, and the disodium salt of SDCDPS precipitated as a white powder. The precipitate was recovered by filtration, dissolved in 400 mL of cold deionized water, and treated with a 2 M solution of NaOH to a pH of 6-7.

Additionally, an excess amount of NaCl (60 g) was added again to salt out the sodium form of the monomer. The final product was filtered and recrystallized from methanol and deionized water (9/1, v/v). The final product had an appearance like white needle crystals.

2.2.2 Synthesis of Sulfone/Ketone Based Random Polymers

The procedure followed to prepare the 25% sulfonated random poly(arylene ether sulfone) (SPAES A 25) or 25% sulfonated random poly(arylene ether ketone) (SPAEK A 25) is presented next (Figure 1). All the monomers were dried before employment. First, 5.5 mmol of BPA, 2.25 mmol of DCDPS or DCBP, 2.5 mmol of SDCDPS or SDCBP (rapidly weighed) were added to a 250 mL three-necked flask with a stirrer, a nitrogen inlet, and a Dean–Stark trap. Potassium carbonate (11.8 mmol) and sufficient DMAc were added to afford a 20% (w/v) solid concentration. Toluene (DMAc/toluene 2/1 v/v) was used as an azeotroping agent. The reaction mixture was refluxed at 150 °C for 4 h to dehydrate the system. The temperature was raised slowly to 165 °C for the controlled toluene removal. The reaction was allowed to proceed for 24 h, and the reaction solution became very viscous. The solution was then cooled to room temperature and diluted with enough DMAc to allow filtering. After filtration, most of the salts were removed, and the copolymer was isolated by coagulation in 2-propanol. The precipitated copolymer was washed several times with deionized water to remove the residual salts. Finally, it was dried at 60 °C for 48 h.



X: C=O or O=S=O

Figure 1: Procedure for the SPAEK 25 and SPAES A 25 random polymer preparation.

2.3 Characterization

2.3.1 Fourier Transform Infrared (FTIR) Spectroscopy

FTIR spectroscopy allows for the qualitative screening of intermediate steps and the final copolymer. Spectrums were obtained employing an ALPHA Platinum Bruker with a diamond ATR holder and a wavenumber range of 500–4000 cm⁻¹, using 100 scans with a 4 cm⁻¹ resolution.

2.3.2 Thermogravimetric Analysis (TGA)

TGA was performed using TA TGA Q50 equipment to study the copolymer membranes' thermal stability. Samples weighing 20-30 mg were heated from 25 °C to 800 °C under a nitrogen atmosphere employing a heating rate of 10 °C min⁻¹.

2.3.3 Oxidative Stability

To evaluate the oxidative stability of the composite membranes, Fenton's test, which consists of an accelerated oxidative degradation method, was performed. From previously dried membranes, duplicates were immersed in 10 ml Fenton's reagent (4 ppm $\text{Fe}(\text{SO}_4)_2 \cdot 7\text{H}_2\text{O}$ in 3 wt % H_2O_2 aqueous solution) at 60 °C for 72 h. Every 24 h, the Fenton solution was replaced, and the residual weight (RW) was measured after removing the excess solution from the sample when the period ended. The RW was calculated using Equation (1)¹¹:

$$RW(\text{wt } \%) = \frac{W_{\text{remaining}}}{W_{\text{initial}}} \quad (1)$$

2.3.4 Ion Exchange Capacity (IEC)

IEC is obtained by immersing pre-dried membranes into 1 M NaCl solution for 24 h. After this period, the membrane is removed from the solution, and the solution is titrated with 0.01 M NaOH solution until neutral pH. The IEC is obtained using the ion mole ratio per dry membrane weight, as shown in Equation (2). Samples were analyzed in triplicates.

$$\text{IEC} \left(\frac{\text{mequiv.}}{\text{g}} \right) = \frac{V_{\text{NaOH}} \times C_{\text{NaOH}}}{W_{\text{dry}}} \quad (2)$$

2.3.5 Water Uptake, Swelling Ratio, and Water Content

The weight difference between dry and wet membranes provides water uptake. First, dry membranes are weighed and placed into deionized water for 24 h at room temperature.

Then the wet membrane is blotted dry and weighed again. Water uptake is obtained by employing equation (3). Samples were analyzed in triplicates.

$$\text{Water uptake (\%)} = \frac{W_{wet} - W_{dry}}{W_{dry}} \times 100 \quad (3)$$

Water content (λ) describes the number of water molecules surrounding an ionic domain. It is calculated using Equation (4).

$$\lambda = \frac{10 \text{ Water Uptake}}{18 \text{ IEC}} \quad (4)$$

2.3.6 Atomic Force Microscopy (AFM)

Phase images of the membranes were obtained employing an Agilent AFM 550 in AC imaging mode at room temperature. Silicon scanning probe microscopy cantilevers for the noncontact test were employed. Measurements were performed for dry membrane samples and 48 h hydrated samples. All images were obtained with a resolution of 256 and a scanning speed of 2.01 lines s⁻¹.

2.3.7 Small Angle X-ray Scattering (SAXS)

The Small-angle X-Ray scattering (SAXS) technique was used to analyze morphological differences between the samples and to determine the interstitial distance between atoms. The experiments were performed on dried samples under a vacuum at 25 °C and with an X-ray exposure time of 1 min. The SAXS profiles of the samples were obtained normal to the plane of the membranes using a SAXSpace (Anton Paar) system with CuK α as the radiation source operated at 50 mA and 40 kV. The scattering patterns were

collected using image plates as detectors and a Cyclone[®] Plus PerkinElmer image plate reader. Then, the data were corrected and converted to one-dimensional intensity using SAXStreat software[®] and SAXSQuant software[®], respectively.

The interstitial distance between atoms was calculated using Bragg's law (Equation 5), where d is the distance between atoms and q is the scattering vector. ¹²

$$d = \frac{2\pi}{q} \quad (5)$$

2.3.8 Proton Conductivity, Effective Proton Mobility, and Methanol Permeability

Proton conductivity (σ) was obtained using a Fuel Test System, 850e multi-Range, equipped with an 885 Fuel Cell Potentiostat from Scribner Associates Inc. Aviles and Suleiman¹³, and Pérez and Suleiman¹⁴ previously reported the procedure. Proton conductivity, σ , is calculated by Equation (6), where L (cm) is the membrane thickness and A (cm²) is the membrane area. Real impedance (Ω) is obtained from the x-intercept of the Nyquist plot.

$$\sigma \left(\frac{S}{cm} \right) = \frac{L}{AR} \quad (6)$$

Once proton conductivity is calculated, the effective proton mobility (μ_{eff}), Equation (7), can be then found using the [ionic domain], Faraday's constant (F), and σ .

$$\mu_{\text{eff}} \left(\frac{cm^2}{sV} \right) = \frac{\sigma V_{\text{wet}}}{FW_{\text{dry}} IEC} \quad (7)$$

Methanol permeability (P) is measured at room temperature using a side-by-side diffusion cell. Previously hydrated membranes are placed between the two compartments of the

cell. The donor compartment is filled with a 2 M methanol solution, while the acceptor compartment is filled with DI water. The concentration of methanol is obtained using FTIR by monitoring the C-O stretch at 1014 cm⁻¹, and the permeability coefficient is obtained from the slope $\frac{C_B(t)V_B L}{C_A A}$ vs. t. Diffusion in-plane sheet geometry approximation (Equation (8)**Error! Reference source not found.**) is used at this expense. Here C_A (M) and C_B(M) are Methanol concentration at donor and acceptor compartments, respectively, L is the membrane thickness (cm), A is the membrane cross-sectional area (cm²), D is methanol diffusion coefficient (cm²/s), and P (cm²/s) is the permeability.

$$\frac{C_B(t)V_B L}{C_A A} = P \left(t - \frac{L^2}{6D} \right) \quad (8)$$

Once the proton conductivity and methanol permeability values are obtained, the selectivity of the membranes is calculated by taking the proton conductivity over the methanol permeability ratio. The membrane selectivity is normalized using the reported values for the state-of-the-art commercial Nafion[®] 117 at 50 °C, as shown in (9).

$$\alpha^* = \frac{\left(\frac{\sigma}{P_{MeOH}} \right)_{membrane}}{\left(\frac{\sigma}{P_{MeOH}} \right)_{Nafion\ 117^{\circ}}} \quad (9)$$

3.0 Results

3.1 Fourier Transform Infrared (FTIR) Spectroscopy

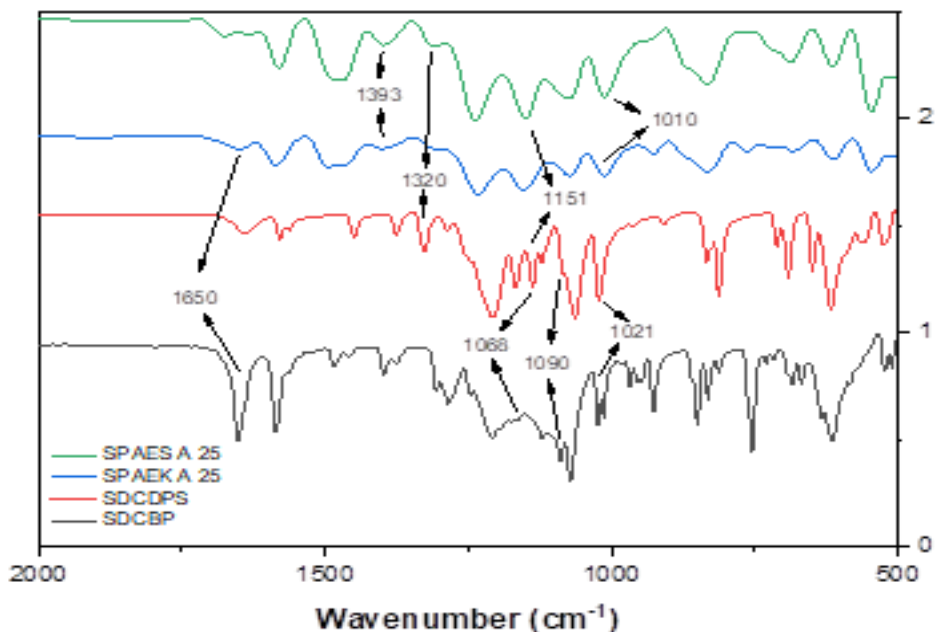


Figure 2: FTIR spectrum of random sulfone and ketone 25% sulfonated polymers. Starting from the sulfonated units (SDCDPS and SDCBP), the signals at 1021 and 1090 cm^{-1} were assigned to the SO_3Na group's symmetric and asymmetric stretching.⁷ Stretching signal at 1168 cm^{-1} also confirm the units' sulfonation.¹⁵ The 1010 cm^{-1} band on the SPAES A 25 and SPAEK A 25 polymers confirm the creation of the arylene-oxygen-arylene bonds, which supports incorporating the sulfonated and non-sulfonated units. From this analysis also, the isopropyl signal corresponding to the BPA unit is present at 1393 cm^{-1} .¹⁶ Ketone and sulfone characteristic bands are identified at ~ 1650 cm^{-1} for the C=O stretch and at 1308 and 1151 cm^{-1} , corresponding to the symmetric and asymmetric stretch of O=S=O groups. Additional signals for these polymers can be observed in Figure 2.

3.2 Thermogravimetric Analysis (TGA)

The TGA technique studied the thermal stability of the synthesized polymers. The spectra showed five main transitions for the sulfone-based polymer and four for the ketone-based (Figure 3 and Table 1). Transitions below 300 °C for these polymers are related to the decomposition of the sulfonic groups. The transitions near 400 °C can be associated with the degradation of aliphatic groups from BPA. Interestingly the degradation of sulfonic groups on SPAES A 25 occurs in three steps compared to SPAEK A 25. These degradation steps may suggest increased ionic domain interactions that protect these groups from a single-step degradation, as observed in sulfonated SIBS, or a two-step degradation, as observed in the ketone-based polymer. Transitions at 498 °C and 484 °C, correspond to thermal degradation of the polymer backbone for SPAES A 25 and SPAEK A 25, respectively.¹⁰ In this last step, a 14 °C difference is also present for the backbone degradation of the sulfone-based polymer, which supports that sulfones on the polymer play a stable role for the polymeric main chain. At 500 °C, both materials remain over 50% of their initial weight, which makes them good candidates for PEMFC at elevated temperatures.

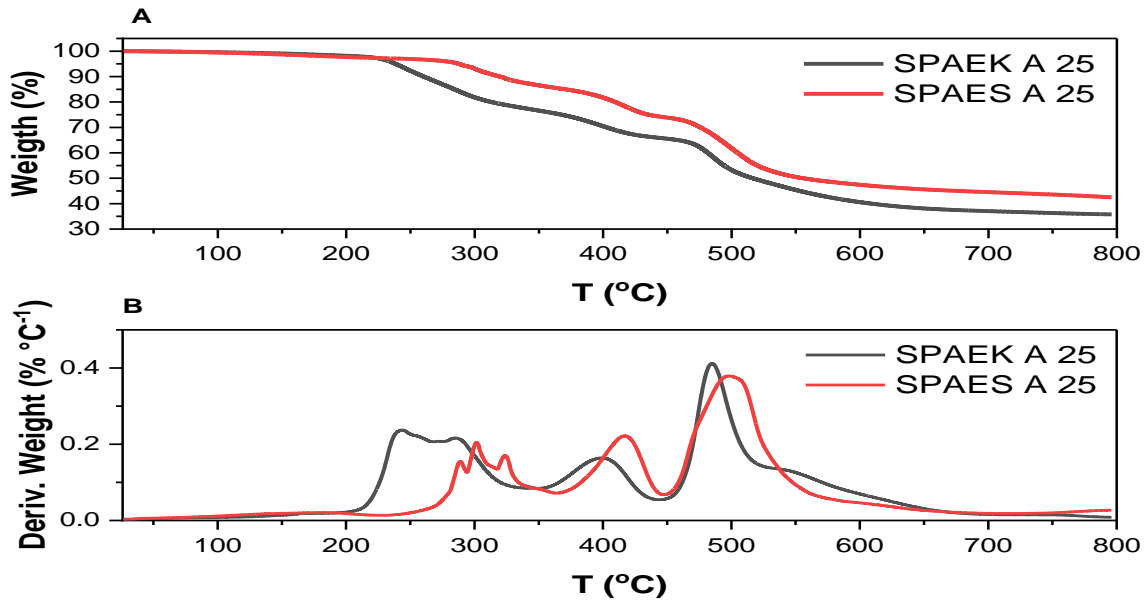


Figure 3: TGA and derivative plots of random sulfone and ketone 25% sulfonated polymers.

Table 1: Thermal transition temperatures for SPAES A 25 and SPAEK A 25 polymers.

Polymer	Degradation temperatures (°C) based on Derivative Weight (%/°C)					50% weight loss T (°C)	Remaining weight (%) at 800 °C
	T 1	T 2	T 3	T 4	T 5		
SPAEK A 25	242.68	288.25	400.18	484.15	-	516	35.80
SPAES A 25	281.25	297.15	317.39	407.74	498.11	554	42.51

3.3 Oxidative Stability

After performing the Fenton test for the random polymers, the observed results were very interesting (Table 2). The sulfone-based polymer was destroyed by the action of the oxidative species, while the ketone-based polymer retained approximately 89% of its initial weight. Structurally, the most crystalline behavior of the ether ketone plays a protective role for the polymer. From water capabilities analysis, the difference in water uptake from the polymers may explain the remaining weight results. The sulfone-based

polymer water uptake was three times higher than the ketone polymer. This behavior implies that oxidative species could have had more access to the polymer matrix, facilitating the attack of carbon linkages. Additionally, the ion exchange capacity difference between the polymers is related to the oxidative attack effectivity due to the aqueous Fenton's reagent's swelling of the ionic groups.¹⁷

Table 2: Remaining weight (%) after 72 h for random SPAEK A 25 and SPAES A 25 polymers at 60 °C.

Polymer	Remaining weight (%) after 72 h at 60 °C
SPAEK A 25	88.90 ± 3.40
SPAES A 25	0.00

3.4 Ion Exchange Capacity (IEC), Water Uptake, and Water Content

IEC, water uptake, and water content tests were performed for the two prepared polymers, and the results are shown in Figure 4. Starting with the water uptake, a clear difference in the behavior of both polymers is observed. Sulfone-based polymer presents three times the ability to absorb water than ketone polymer. From a chemical structure view, sulfone-based polymers are more suitable for hydrophilic candidates because they form more hydrogen bonds with water than ketones.^{18,19} Oroujzadeh and Mehdipour-Ataei reported that the presence of sulfone groups on a polymeric backbone lowers the general density of the polymer, allowing more solvent interactions in a limited space.²⁰ In addition, the previously described factors become exacerbated by the action of sulfonic groups, even when low sulfonations are achieved.

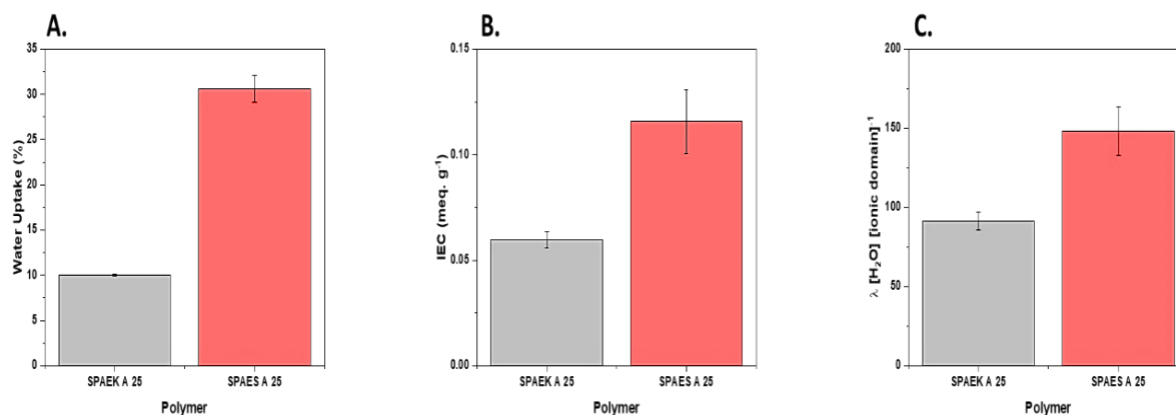


Figure 4: A. Water uptake values, B. Ion exchange capacity, and C. Water content for random ketone and sulfone-based polymers.

Figure 4-B presents the ion exchange capacity for the synthesized polymers. Two possible explanations are considered. First, the ionic domains are inaccessible to counter-ion substitution in the IEC experiment. The second potential explanation is that the pre-sulfonated units possibly were not fully sulfonated. Additionally, the presence of ionic domains that cannot exchange protons influences the test outcome, making it a sulfonation degree underestimation tool. For example, Yang and Manthiram prepared a series of 44 to 58% sulfonated poly(ether ketones). For their results, IEC values ranged from 1.36 to 1.74 meq. g⁻¹, but its maximum water uptake was 5.3%. Interestingly the obtained conductivity was lower than Nafion[®] at 80 °C, which supports the rationale expressed above.²¹

The water uptake and ion exchange capacity of the membranes led to calculating the water content per ionic domain on the membranes (Figure 4-C). Similarly to the previous two tests, the sulfone-based polymer presented a higher water content than the ketone-based polymer. The λ values represent a complex number often used to predict high proton conductivities. As a general rule, proton conductivity increases with λ values as it

is bound to the ionic domains and helps with the proton conduction process. However, there is a limit where elevated water content on the membrane becomes simply bulk water incapable of allowing for proton transport, thus dissolving the available acid sites for conduction.²²

3.5 Atomic Force Microscopy (AFM)

The analysis of phase segregation on a given material can be done using the AFM technique. According to the results (Figure 5), there appear to be two distinct phase segregation patterns. First, a clear distinction between hydrophilic (dark regions) and hydrophobic (bright regions)²³ was found for a 25 μm scan size (Figure 5-A & C). The results agree with the water uptake values given that the ketone-based polymer has an intercalated-like shape at this scale. These findings also support the outcomes of its oxidative breakdown and the differences in the polymers' water absorption capabilities.

For the small scan area (100 x 100 nm), the obtained image is more even in appearance. This result is a suggestion of a poor-segregated microphase; however, a slight difference could be observed when comparing Figure 5-B & D. In Figure 5-B, the hydrophilic domains appear to be concentrated on the upper part of the image, separated by hydrophobic continuous sections, giving the idea of a general intercalated phase even at the smaller scale. On the other hand, Figure 5-D presents the hydrophilic domains more evenly distributed across the area, even when no interconnection can be appreciated. These findings, combined with the water absorption tests, explain why sulfone-based

polymers present a more suitable scenario for higher proton conductivity than ketone-based polymers.²⁴

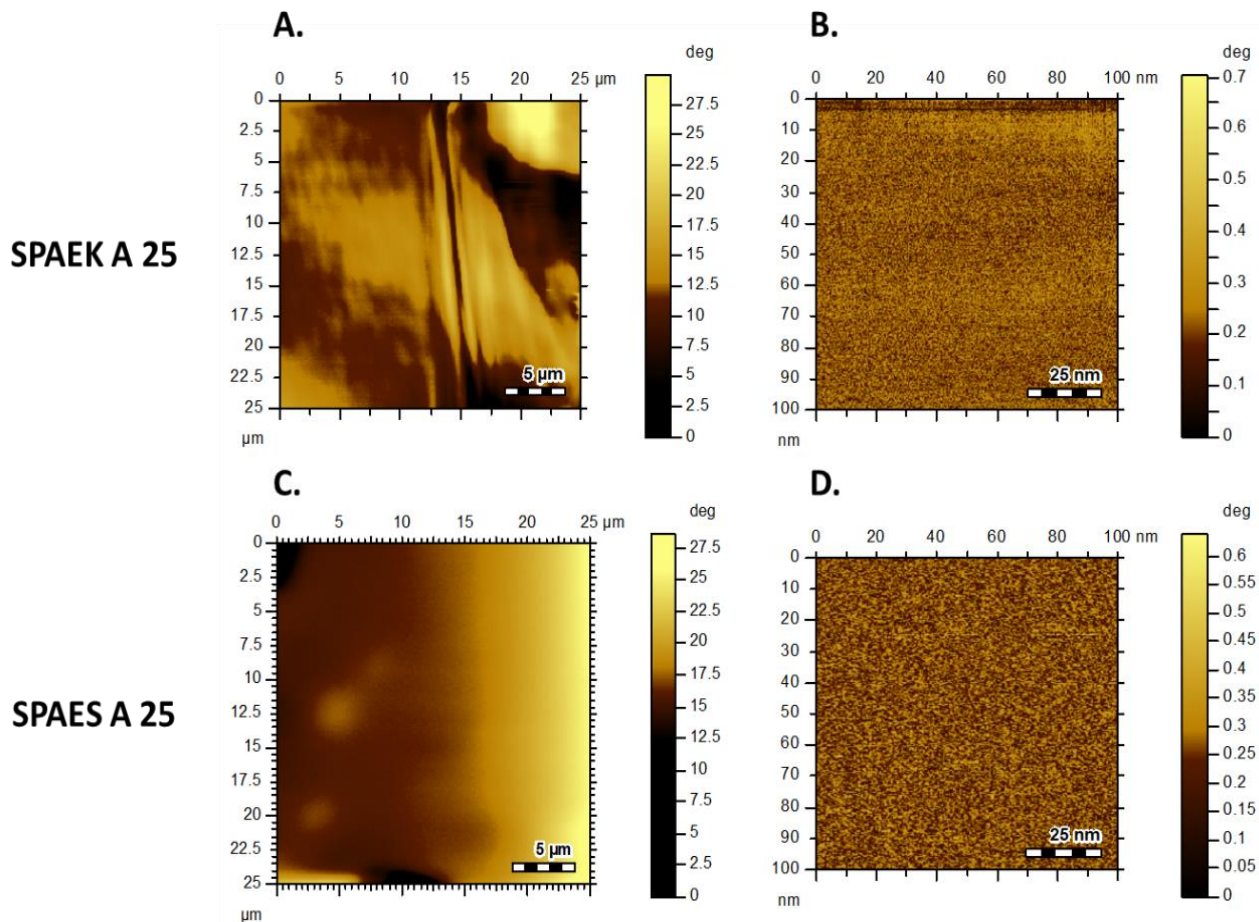


Figure 5: AFM images for SPAEK A 25; A. 25 μm and B. 100 nm and SPAES A 25; C. 25 μm and D. 100 nm.

3.6 Small Angle X-ray Scattering (SAXS) and Wide Angle X-ray Scattering (WAXS)

SAXS analysis found two characteristic peaks for both random polymers (see Figure 6). First, two distinct peaks on the 0.1-0.2 nm⁻¹ region resulted in Bragg's 42.34 nm and 50.72 nm distances for the ketone and sulfone polymers, respectively. Additionally, two

peaks appear on the 8-16 nm⁻¹ WAXS region, almost the same as the first. Bragg's distance regarding these peaks is 0.4841 and 0.49 nm for ketone and sulfone polymers, respectively (see Table 3). From a chemical structure perspective, the first peaks are attributed to the characteristic ionomers on the polymer, biphenyl ketones or sulfones, separated by BPA units. The elevated poly(ketone)s crystallinity has been widely reported over poly(sulfone)s.^{25,26} Despite this fact, the synthesis route chosen for this work obligates the presence of a BPA unit between dichloro ketone/sulfone units, indistinctly sulfonation. This is why the characteristic ionomer mean distance was comparable, although the two polymers possess important structural differences.

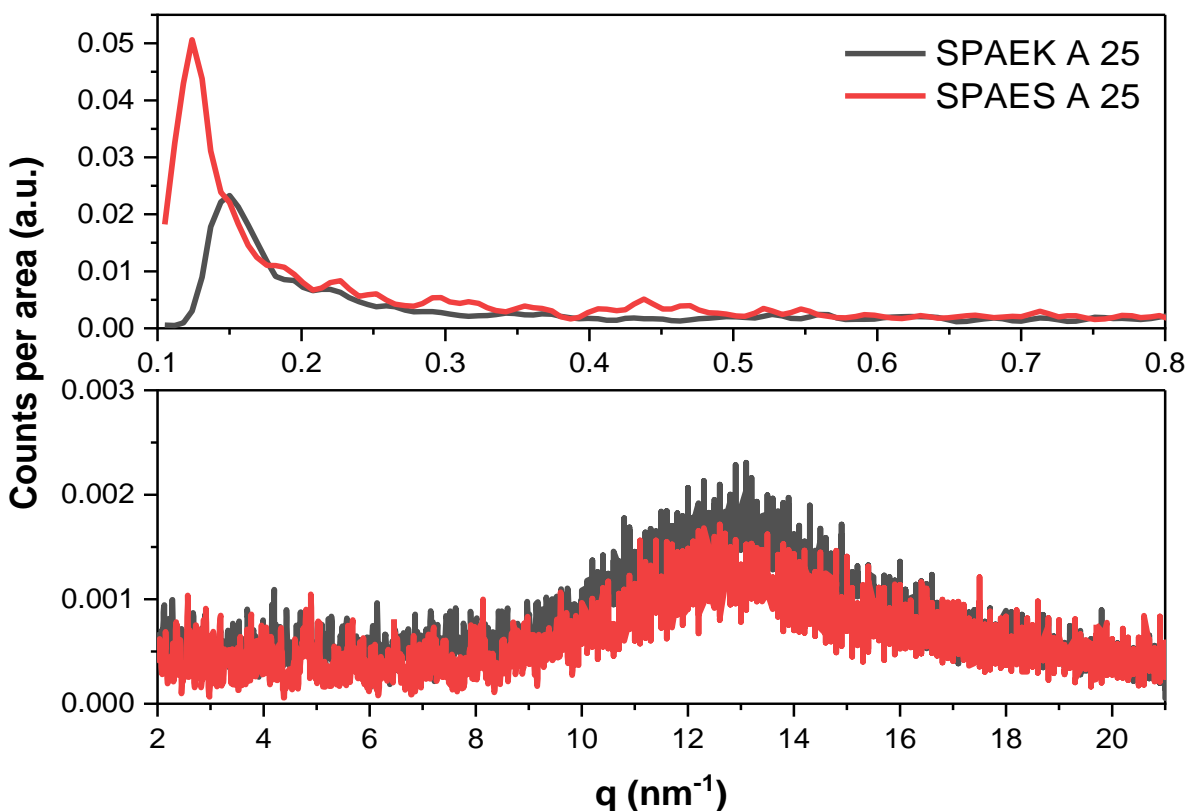


Figure 6: SAXS/WAXS profiles for random sulfone and ketone 25% sulfonated polymers.

Table 3: Scattering vector (q) and Braggs distance (d) for random sulfone and ketone 25% sulfonated polymers

Polymer	q_1 (nm^{-1})	d_1 (nm)	q_2 (nm^{-1})	d_2 (nm)
SPAEK A 25	0.15	42.34	12.97	0.48
SPAES A 25	0.12	50.72	12.75	0.49

Interestingly, from the second Bragg's distance, it could be stated that this mean distance represents the SO_3H group separation, which represents the sulfonated units distributed across the polymer's backbone.^{27,28} From these results, it is important to point out the similarities in the peak intensity for SPAEK A 25 and SPAES A 25, indicative of the sulfonation similarities. However, regarding phase segregation, the SO_3H mean separation being shorter, could indicate a less phase-segregated membrane.

Another important consideration is the packing of the polymeric structure. Due to the rigid nature of the poly(arylene ether) polymers, they are expected to have smaller ionic clusters, like those found in SAXS analysis (Table 3). The cluster size reported for SPEEK is about 1 nm and 5 nm for Nafion[®].^{29,30} When we compare our cluster size with SPEEK and Nafion[®], it is possible to suggest that the obtained results <0.50 nm for the studied polymers may take an important role in the presence of distributed water across the membrane. Even when the structure of the ketone and sulfone-based polymers is quite the same, the sulfone presence alters the packing trend of the backbone. Because of this alteration, the combination of interactions between ionic groups promotes a higher water content across the backbone, which creates a more suitable environment for proton conduction.

3.7 Proton Conductivity, Effective Proton Mobility, and Methanol Permeability

The transport properties of the studied polymers are presented in Figure 7. As expected, the proton conductivity (Figure 7-A) was higher for the sulfone based-polymer at both studied temperatures. The better phase segregation for the SPAES A 25 polymer favored the proton conductivity over the SPAEK polymer and Nafion[®] 117.³¹ It has been previously reported that Nafion[®] possesses a lamellar structure separating the hydrophobic domains, allowing an improved interconnection of its hydrophilic groups.³² From the AFM results is more feasible to expect a better-organized phase for the sulfone polymer, favoring the water presence near the ionic conducting groups and, therefore, proton conduction.

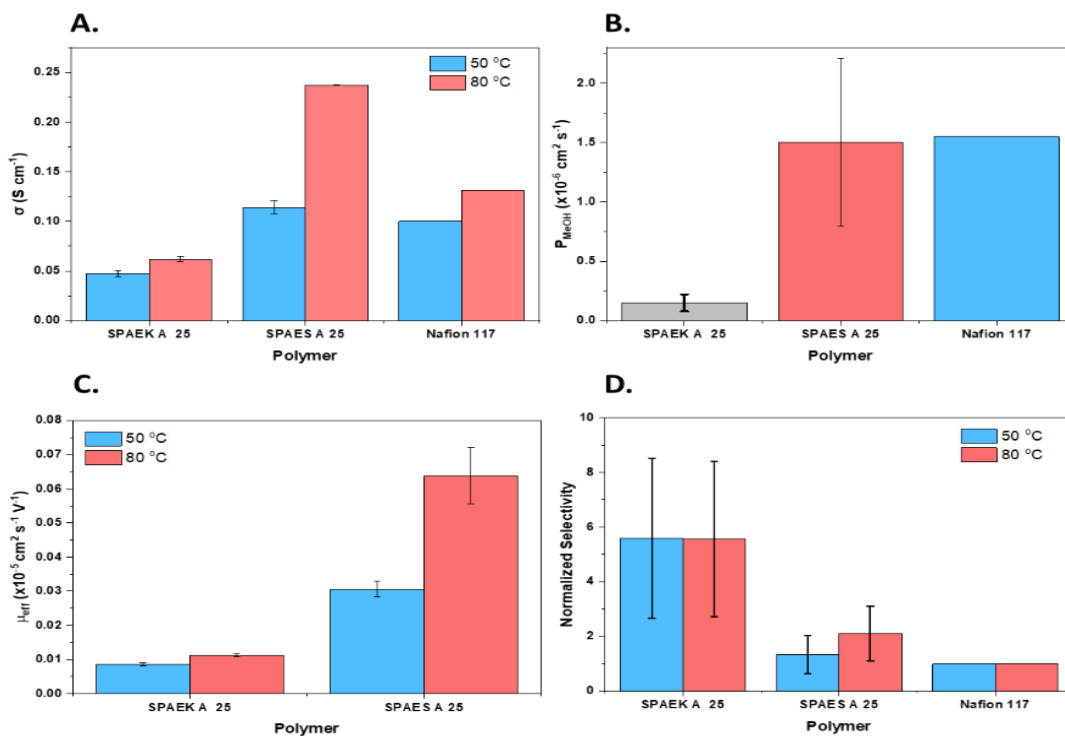


Figure 7: Transport properties for random SPAEK A 25 and SPAES A 25 polymers. A. Proton conductivities at 50 °C and 80 °C (data for Nafion[®] 117 obtained from Kang & Kim, 2015³¹), B. Methanol permeability (Data for Nafion[®] 117 obtained from Wang et al., 2011)³³, C. Effective proton mobility and D. Normalized selectivity using Nafion[®] 117.

From water absorption tests (Figure 4), the obtained λ values showed differences for the studied polymers. However, despite the higher water content observed for sulfone polymer, both materials follow the vehicular proton transport mechanism.³⁴ This result has important implications for effective proton mobility, which measures the tortuosity of the ionic channels. As observed for proton conduction, the results were higher for the SPAES A 25 polymer achieving its peak with a $6.55 \times 10^{-5} \text{ cm}^2 \text{ s}^{-1} \text{ V}^{-1}$ at 80 °C (Figure 7-C). Having similar sulfonic groups distance (Table 3), the results from the intercalated morphology (Figure 5) support a greater tortuosity for the protons to travel through the ketone polymeric matrix. When compared, the effective proton mobility results with Nafion® NR-211 reported values at 50 °C and 80 °C (5×10^{-4} and $8 \times 10^{-4} \text{ cm}^2 \text{ s}^{-1} \text{ V}^{-1}$, respectively).³⁵ This comparison supports the morphological impedance both polymeric structures present to the proton mobilities, particularly in the ketone polymer case.

When analyzing the random polymers' methanol permeability, both obtained results in the $10^{-6} \text{ cm}^2 \text{ s}^{-1}$ range. However, the most remarkable permeability for the ketone polymer was less than $0.25 \times 10^{-6} \text{ cm}^2 \text{ s}^{-1}$. The results obtained for SPAEK A 25 are concordant with reported values for SPEEK, which are lower than those for Nafion®.³⁶ As a possible explanation for this behavior, perfluorinated polymers have a highly hydrophobic backbone and an incredibly large hydrophilic sulfonic group composition in their microstructure. In this structure, sulfonic groups gather to form ion clusters in water's presence, creating well-connected water channels. The SPAEK A 25 membrane's main chain is less hydrophobic, and the sulfonic acid group is less acidic than the Nafion® membrane. Because of this, there is less nano-separation and a bigger hydrophobic-hydrophilic interface corresponding to highly dispersed sulfonic groups through the

backbone. As a result, compared to Nafion[®] membranes, the water-filled channels of SPAEK A 25 membrane are more branched and present more dead-end pockets.^{24,37} With all the findings on transport properties, the membranes' selectivity can be observed in Figure 7-D. The best selectivity was obtained for the SPAEK A 25, achieving values near 5.8. Interestingly, the temperature does not appear to affect the performance of the membrane in terms of selectivity. For the SPAES A 25 polymer, the temperature seems to have an effect, achieving the highest selectivity at 80 °C (2). Both studied polymers presented a selectivity superior to Nafion[®] 117; however, considering the thermal stability, proton conductivity, and comparable methanol permeability with Nafion[®], SPAEK A 25 could be a viable candidate for DMFC, but increasing its oxidative stability.

4.0 Conclusions

Using the pre-sulfonation approach, two random poly(arylene ether) sulfone and ketone polymers were synthesized with 25% sulfonation. FTIR and TGA analysis confirmed the presence of the main groups and structure for SPAEK A 25 and SPAES A 25 polymers. Both polymers showed excellent thermal properties up to 500 °C retaining more than 50% of their initial weight. From the oxidative resistance test, SPAEK A 25 was extremely resistant, maintaining more than 88% of its initial weight before three days at 60 °C. Two main structural regions were identified by SAXS analysis resulting in 42 and 50 nm characteristic ionomer distances for SPAEK A 25 and SPAES A 25, respectively, with ~0.49 nm sulfonic domains distance for both polymers. Morphological microstructure differences were observed between the polymers because the ketone-based material is more intercalated than the sulfone polymer.

The transport properties were highly affected by the water management of the materials; the SPAES A 25 membranes had the most water absorption and better proton conducting at 80 °C (0.24 S cm⁻¹). On the other hand, the methanol permeability was better controlled by the SPAEK A 25 membranes, achieving values lower than 0.25 x10⁻⁶ cm² s⁻¹. The selectivity of both polymers exceeded the reported values for Nafion[®] 117, and both could be viable candidates for DMFC applications. However, it is worth mentioning the outstanding proton conductivity of SPAES A 25, due to synergistic effects between sulfonic, sulfone and ether domains with proper water management. Similarly, it is important to emphasize the outstanding barrier properties and oxidative stability of SPAEK A 25.

5.0 References

1. Wang, Z.; Ni, H.; Zhao, C.; Li, X.; Zhang, G.; Shao, K.; Na, H. *J. Membr. Sci.* **2006**, *285*, 239.
2. Wang, F.; Chen, T.; Xu, J.; Liu, T.; Jiang, H.; Qi, Y.; Liu, S.; Li, X. *Polymer* **2006**, *47*, 4148.
3. Lakshmi, R. T. S. M.; Meier-Haack, J.; Schlenstedt, K.; Komber, H.; Choudhary, V.; Varma, I. K. *React. Funct. Polym.* **2006**, *66*, 634.
4. Robeson, L. M.; Matzner, M. Flame retardant polyarylate compositions **1983**.
5. Sankir, M.; Bhanu, V. A.; Harrison, W. L.; Ghassemi, H.; Wiles, K. B.; Glass, T. E.; Brink, A. E.; Brink, M. H.; McGrath, J. E. *J. Appl. Polym. Sci.* **2006**, *100*, 4595.
6. Li, Y.; VanHouten, R. A.; Brink, A. E.; McGrath, J. E. *Polymer* **2008**, *49*, 3014.
7. Wang, F.; Hickner, M.; Ji, Q.; Harrison, W.; Mecham, J.; Zawodzinski, T. A.; McGrath, J. E. In *Macromolecular Symposia*; Wiley Online Library, **2001**; Vol. 175, pp 387.
8. Pirali-Hamedani, M.; Mehdipour-Ataei, S. *Des. Monomers Polym.* **2017**, *20*, 54.
9. Wang, B.; Hong, L.; Li, Y.; Zhao, L.; Wei, Y.; Zhao, C.; Na, H. *ACS Appl. Mater. Interfaces* **2016**, *8*, 24079.
10. Liu, C.; Wang, X.; Xu, J.; Wang, C.; Chen, H.; Liu, W.; Chen, Z.; Du, X.; Wang, S.; Wang, Z. *Int. J. Hydrog. Energy* **2020**, *45*, 945.
11. Ruiz-Colón, E.; Pérez-Pérez, M.; Suleiman, D. *J. Appl. Polym. Sci.* **2019**, *136*, 47009.
12. Barrios-Tarazona, K.; Suleiman, D. *J. Appl. Polym. Sci.* **2021**, *138*, 50034.

13. Avilés-Barreto, S.; Suleiman, D. *J. Appl. Polym. Sci.* **2013**, *129*, 2294.
14. Pérez-Pérez, M.; Suleiman, D. *J. Appl. Polym. Sci.* **2016**, *133*.
15. Sutradhar, S. C.; Ahmed, F.; Ryu, T.; Yoon, S.; Lee, S.; Rahman, M. M.; Kim, J.; Lee, Y.; Kim, W.; Jin, Y. *Int. J. Hydrog. Energy* **2019**, *44*, 11321.
16. Fei, B.; Chen, C.; Peng, S.; Zhao, X.; Wang, X.; Dong, L. *Polym. Int.* **2004**, *53*, 2092.
17. Oishi, A.; Matsuoka, H.; Yasuda, T.; Watanabe, M. *J. Mater. Chem.* **2009**, *19*, 514.
18. Mohammad, A. W.; Teow, Y. H.; Chong, W. C.; Ho, K. C. In *Membrane Separation Principles and Applications*; Ismail, A. F.; Rahman, M. A.; Othman, M. H. D.; Matsuura, T., Eds.; Handbooks in Separation Science; Elsevier, **2019**; pp 401.
19. Fan, G.; Su, Z.; Lin, R.; Lin, X.; Xu, R.; Chen, W. *Int. J. Polym. Sci.* **2016**, *2016*, e6895235.
20. Oroujzadeh, M.; Mehdipour-Ataei, S. *Polym. Adv. Technol.* **2022**, *33*, 2896.
21. Yang, B.; Manthiram, A. *Electrochem. Solid-State Lett.* **2003**, *6*, A229.
22. Peckham, T. J.; Schmeisser, J.; Rodgers, M.; Holdcroft, S. *J. Mater. Chem.* **2007**, *17*, 3255.
23. Wang, F.; Hickner, M.; Kim, Y. S.; Zawodzinski, T. A.; McGrath, J. E. *J. Membr. Sci.* **2002**, *197*, 231.
24. Kreuer, K. D. *J. Membr. Sci.* **2001**, *185*, 29.
25. Cho, S.; Lee, J. S.; Jang, H.; Park, S.; An, J. H.; Jang, J. *Polymers* **2021**, *13*, 919.
26. Klop, E. A.; Lommerts, B. J.; Veurink, J.; Aerts, J.; Van Puijenbroek, R. R. *J. Polym. Sci. Part B Polym. Phys.* **1995**, *33*, 315.
27. Mendil-Jakani, H.; Lopez, I. Z.; Legrand, P. M.; Mareau, V. H.; Gonon, L. *Phys. Chem. Chem. Phys.* **2014**, *16*, 11243.
28. Chen, R.; Jin, J.; Yang, S.; Li, G. *J. Mater. Sci.* **2017**, *52*, 1028.
29. Pineri, M.; Gebel, G.; Davies, R. J.; Diat, O. *J. Power Sources* **2007**, *172*, 587.
30. Yang, B.; Manthiram, A. *J. Power Sources* **2006**, *153*, 29.
31. Kang, K.; Kim, D. *J. Power Sources* **2015**, *281*, 146.
32. Wu, X.; Wang, X.; He, G.; Benziger, J. *J. Polym. Sci. Part B Polym. Phys.* **2011**, *49*, 1437.
33. Wang, C.; Li, N.; Shin, D. W.; Lee, S. Y.; Kang, N. R.; Lee, Y. M.; Guiver, M. D. *Macromolecules* **2011**, *44*, 7296.
34. Zuo, Z.; Fu, Y.; Manthiram, A. *Polymers* **2012**, *4*, 1627.
35. Peron, J.; Mani, A.; Zhao, X.; Edwards, D.; Adachi, M.; Soboleva, T.; Shi, Z.; Xie, Z.; Navessin, T.; Holdcroft, S. *J. Membr. Sci.* **2010**, *356*, 44.
36. Xue, S.; Yin, G. *Eur. Polym. J.* **2006**, *42*, 776.
37. Mauritz, K. A.; Moore, R. B. *Chem. Rev.* **2004**, *104*, 4535.